Thin Solid Films 604 (2016) 1–6

Contents lists available at ScienceDirect

Thin Solid Films

journal homepage: www.elsevier.com/locate/tsf

Effects of Na incorporation and plasma treatment on Bi_2S_3 ultra-thin layers

H. Moreno-Garcia [a,*], S. Messina [b], M. Calixto-Rodriguez [c], H. Martínez [a]

[a] Laboratorio de Espectroscopía, Instituto de Ciencias Físicas, Universidad Nacional Autónoma de México, Apartado Postal 48-3, 62210 Cuernavaca, Morelos, Mexico
[b] Universidad Autónoma de Nayarit, Ciudad de la Cultura "Amado Nervo" S/N, C.P. 63155 Tepic, Nayarit, Mexico
[c] Universidad Tecnológica Emiliano Zapata del Estado de Morelos, Av. Universidad Tecnológica No. 1, C.P. 62760 Emiliano Zapata, Morelos, Mexico

ARTICLE INFO

Article history:
Received 5 May 2015
Received in revised form 21 November 2015
Accepted 3 December 2015
Available online 31 December 2015

Keywords:
Bismuth sulfide
Thin films
Plasma treatment
Na incorporation

ABSTRACT

As-deposited bismuth sulfide thin films prepared by means of a chemical bath deposition were treated with argon AC plasma. In this paper, we present the results on the physical modifications which were observed when a pre-treatment, containing a solution of 1 M sodium hydroxide, was applied to the glass substrates before depositing the bismuth sulfide. The bismuth sulfide thin films were characterized by X-ray diffraction, energy dispersive X-ray spectroscopy, scanning electron microscopy, atomic force microscopy, UV–VIS, and electrical measurements. The XRD analysis demonstrated an enhancement in the crystalline properties, as well as an increment in the crystal size. The energy band gap value was calculated as 1.60 eV. Changes in photoconductivity (σ_p) values were also observed due to the pre-treatment in NaOH. A value of $\sigma_p = 6.2 \times 10^{-6}\ (\Omega\ cm)^{-1}$ was found for samples grown on substrates without pre-treatment, and a value of $\sigma_p = 0.28\ (\Omega\ cm)^{-1}$ for samples grown on substrates with pre-treatment. Such σ_p values are optimal for the improvement of solar cells based on Bi_2S_3 thin films as absorber material.

1. Introduction

Bismuth sulfide (Bi_2S_3) is part of the semiconductor compound group V–VI. Bi_2S_3 is a typical lamellar-structured semiconductor with a bulk direct band gap of 1.3 eV [1]. In thin-film form, its band gap varies from 1.52 eV to 1.9 eV, depending on the deposition technique. Bi_2S_3 is an n-type semiconductor with remarkable applications in thermoelectric [2,3], optoelectronic [4–6], photo electrochemical [7], and photocatalytic [8] devices.

Methods to improve the physical properties of Bi_2S_3 thin films have been previously conducted by several groups: Rincon et al. [9] reported the annealing of Bi_2S_3 thin films in argon (Ar) or hydrogen at 180 °C to 400 °C and oxygen at 100 °C to 250 °C; Ahire et al. [10] achieved the modifications of the structural, optical, and electrical properties of nanocrystalline bismuth sulfide using swift heavy ions; and recently, we used the post-deposition Ar plasma treatment to enhance the physical properties of the chemically deposited Bi_2S_3 thin films [11].

Another way for improving the physical properties of the thin films is through the incorporation of Na in the absorber layer; such as the case of CIGS-based solar cells [12]. The addition of Na produces an enhancement in the efficiency of the solar cell because of the increase of hole concentration and electrical conductivity of the absorber [13–15], and Na also improves the morphology of the material [16,17] and the grain size [17,18].

The main objective of this paper is to demonstrate that the physical and chemical properties of the Bi_2S_3 films are improved by using a pre-treatment of the substrates in NaOH before the Bi_2S_3 deposition and post-deposition treatment by Ar plasma irradiation in order to use such films in the development of optoelectronic devices and solar cells.

2. Experimental details

2.1. Pre-treatment substrates

Glass substrates were pre-treated by an immersion in a 1 M NaOH (J.T. Baker) solution for 18 h at room temperature. Afterwards, they were rinsed with water and dried with hot air. Subsequently, they were placed into a beaker containing the reaction solution of the Bi_2S_3 chemical bath.

2.2. Bi_2S_3 thin films

The reaction solution and deposition conditions were performed by following the method disclosed by Nair et al. [19]. A solution containing 10 ml of 0.5 M bismuth nitrate dissolved in triethanolamine (TEA) was used for the deposition of the Bi_2S_3 films; de-ionized water was added to 8 ml of 1 M thioacetamide to obtain a total volume of 100 ml [20].

* Corresponding author at: Instituto de Ciencias Físicas, UNAM, C.P. 62210, Mexico.
E-mail address: hamog@ier.unam.mx (H. Moreno-Garcia).

http://dx.doi.org/10.1016/j.tsf.2015.12.011
0040-6090/

The Bi_2S_3 film thickness reached approximately 96 nm after a deposition time of 75 min.

2.3. Plasma treatment

The system is comprised of two circular, copper electrodes that are 80 mm in diameter and have a gap spacing of 3 mm. Electrodes were settled horizontally along the center of the reaction chamber. The samples were placed over the bottom electrode. The plasma chamber was evacuated at a gas pressure of 2×10^{-2} Torr and purged several times using Ar at a pressure of 1.0 Torr in order to remove the background gases. Ar gas was injected into the chamber at a pressure of 3 Torr in order to generate the plasma. The AC discharge power supply was maintained at 290 V and with a current of 64 mA. The samples were treated for 75 min.

Based on the study carried out by Nair et al., which suggests that the use of Ar in heat treatment improves the physical properties of the Bi_2S_3 film [9], we decided to employ an Ar plasma for this research.

The Bi_2S_3 thin films presented in this work were labeled as follows: (A) as-prepared films, (B) as-prepared samples with a pre-treatment in NaOH, (C) samples treated with Ar plasma, and (D) samples deposited on glass substrates with a pre-treatment in NaOH and post-deposition treatment in Ar plasma.

3. Characterization

The X-ray diffraction (XRD) patterns of the resulting Bi_2S_3 thin films were measured using a Rigaku Ultima IV diffractometer in grazing incident mode ($\Omega = 1°$). The crystal size was calculated using the computer software PDXL. Film thickness was recorded using an Ambios Technology XP-200. An atomic force microscope (Dimension Icon model DS100) was employed for morphology analyses. The NanoScope Analysis software version 1.4 was used for calculating the root mean square roughness. The elemental analysis of the films was conducted with a Hitachi SU1510 scanning electron microscope attached to an Oxford energy dispersive, and Inductively Coupled Plasma Optical Emission Spectral (ICP-OES) HORIBA spectrometer to determine the presence of the elements Na, Bi, and S. The transmission (T) and specular reflection (R) spectra of the samples were measured in the UV–VIS-NIR region (200–1100 nm) using a Shimadzu UV1800 spectrophotometer. The optical absorption coefficient (α) was calculated from the T and R spectra and film thickness. The semiconductor energy band gap (E_g) was determined by measuring the absorption coefficient as a function of the photon energy [20]. For the electrical characterization of the samples, two silver electrodes were painted on the surface of the films (5 mm long and 5 mm apart). The films were stabilized in a dark environment before taking the photo response measurements. Thereafter, a bias voltage of 5 V was applied to the films and the electrical current was measured for 30 s in the dark, 30 s under illumination with an intensity of 850 W/m^2 (tungsten–halogen radiation; temperature of 3300 K), and again for 30 s in the dark. Electrical current data was acquired for each second utilizing a measurement system comprised a Kiethley 230 programmable voltage source and Keithley 619 digital multimeter connected to a computer. The electrical conductivity in the dark and light was determined using the photo response data from each film [21]. The hot point probe technique was used to define the conductivity type of the Bi_2S_3 thin films.

4. Results and discussion

The thickness measurements of the films are as follows: 96 nm for the as-prepared film (sample A), 100 nm for the as-prepared film on glass substrates with a pre-treatment in NaOH (sample B), 94 nm for the film treated in Ar plasma (sample C), and 98 nm for the film deposited on glass substrates with a pre-treatment in NaOH and post-deposition treatment in Ar plasma (sample D); as shown in Table 1.

Table 1
Atomic percentages of elemental Na, Bi and S calculated from the EDX measurements.

Sample	Na atomic percentage (%)	Bi atomic percentage (%)	S atomic percentage (%)
Substrate corning	8.6 ± 0.3	0.0	0.0
Substrate corning treated	13.1 ± 0.2	0.0	0.0
A	8.4 ± 0.3	53.4	46.6
B	9.6 ± 0.2	54.6	45.4
C	8.6 ± 0.3	56.0	44.0
D	9.7 ± 0.2	56.1	43.9

4.1. Structural and morphological characterization

Fig. 1 displays the XRD patterns for the Bi_2S_3 ultra-thin films. In our previous work [11], we reported that as-prepared Bi_2S_3 thin films do not exhibit XRD peaks, and for that reason, the XRD measurements for sample A are not included in Fig. 1. Sample B does not reveal any XRD peak or any crystalline structure (amorphous, Fig. 1a). The post-deposition treatment in Ar plasma of the Bi_2S_3 thin films changes the structure from amorphous to crystalline, similar to bismuthinite, with orthorhombic (PDF # 17–0320) crystal structure (Fig. 1b). Fig. 1b and c show that the diffraction planes (020), (120), (220), (310), (211), and (221) exhibit a higher intensity for sample D compared with the XRD peaks of sample C. Additional peaks are detected in the diffraction pattern of sample D in planes (141), (430), (440), and (431).

The estimated values for the crystal size, calculated from the main XRD peak (corresponding to the diffraction plane (310)), for samples C and D are 16.4 nm and 30 nm, respectively. The crystal size for sample D is bigger than that for sample C, therefore indicating a superior crystallization (it occurs when a pre-treatment in NaOH solution is used).

Fig. 2 shows atomic force microscopy (AFM) measurements for a) corning glass, b) corning glass with a pre-treatment in NaOH, c) sample A, d) sample B, e) sample C and f) sample D. The NanoScope Analysis software version 1.4 was used for calculating the root mean square roughness on corning glass and the samples. The roughness of the corning glass was estimated to be 1.1 nm. Surface analysis showed particles with a maximum and minimum diameter value of 27.5 nm and 441.9 nm, respectively. The roughness value of the substrate with NaOH pre-treatment was estimated to be 47.6 nm. Surface analysis showed particles with maximum and minimum diameter values of 1655 nm and 2.29 nm, respectively, and a maximum height of 127 nm. The considerable increase in the roughness is due to the

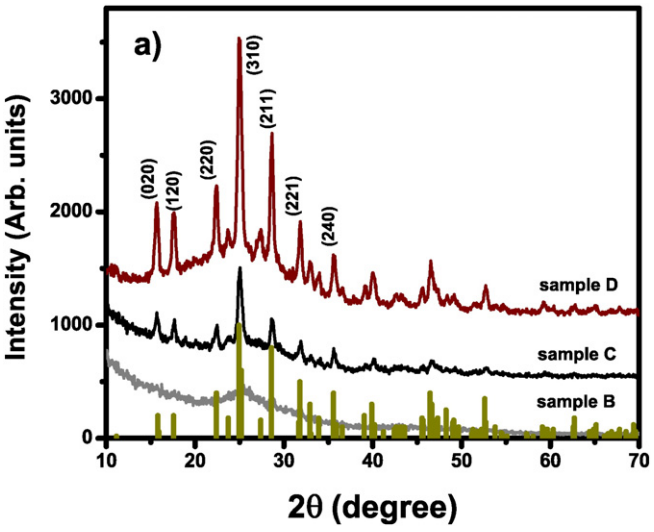

Fig. 1. X-Ray diffraction patterns of Bi_2S_3 thin films: a) Na/as-deposited (sample B), b) treated with Ar plasma (sample C), and c) treated with Na/Ar plasma (sample D).

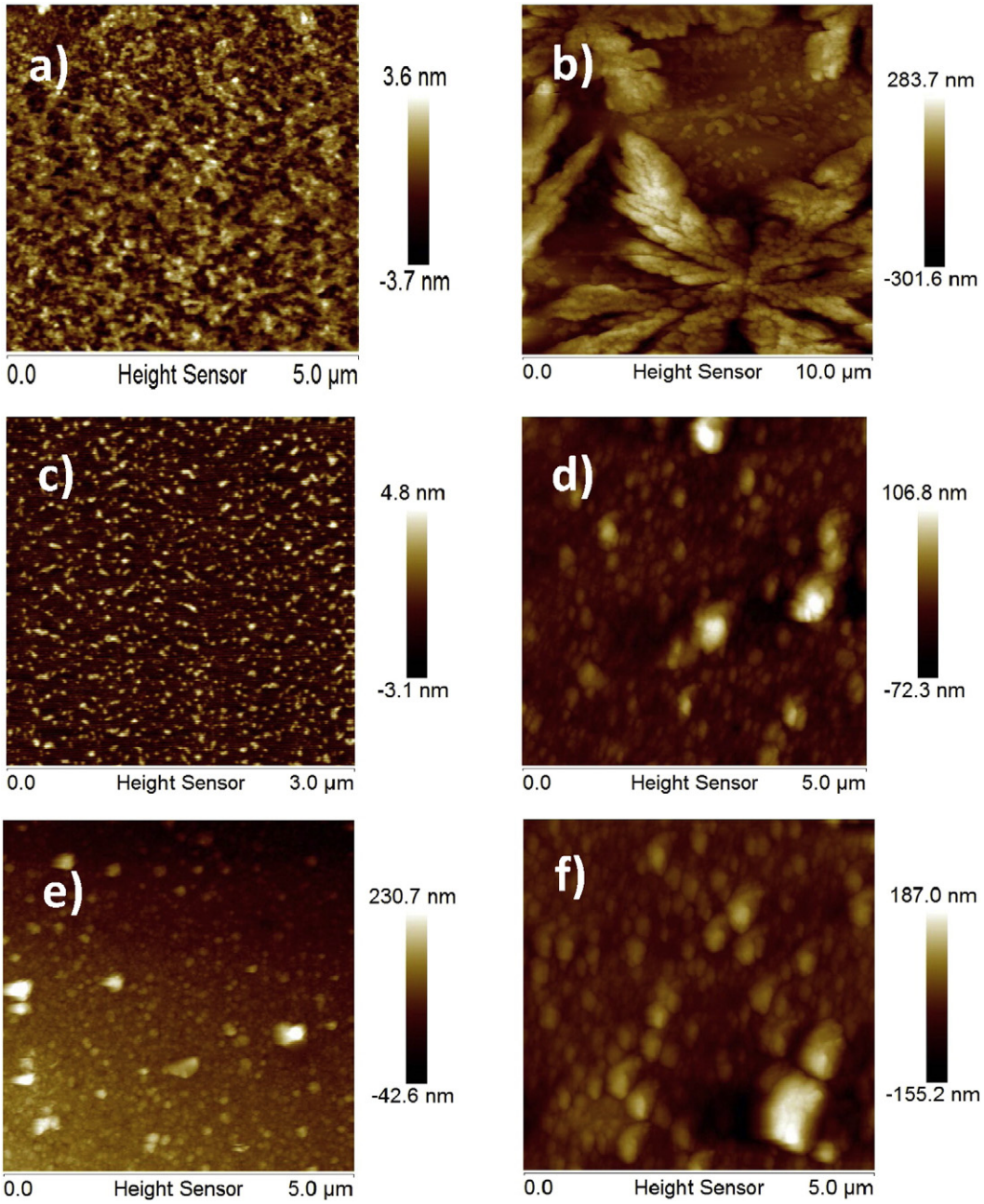

Fig. 2. AFM 2D micrographs for Bi_2S_3 thin films: a) as-prepared (sample A), b) Na/as-prepared (sample B), c) treated with Ar plasma (sample C), and d) treated with Na/Ar plasma (sample D).

presence of multiple NaOH particles adhered to the glass substrate (Fig. B). Sample A displays multiple peaks of less than 6 nm. The roughness value was estimated to be 1.5 nm. The particles in Fig. 2c have an average diameter of 35 nm, a minimum diameter of 33 nm, and a maximum diameter of 386 ± 68 nm. Sample B has a roughness value of 20.4 nm and minimum and maximum diameters of 110 nm and 1500 ± 190 nm. Sample C has a roughness value of 18.5 nm, minimum and maximum diameters of 56.2 and 443 nm, respectively, and a standard deviation of 63.5 nm. Sample D has a roughness value of 21 nm and minimum and maximum diameters of 112 nm and 1600 ± 163.5 nm. Samples pre-treated with NaOH present a slight increase in roughness values compared to samples without pre-treatment, as well as the presence of larger diameter particles. The formation of a non-uniform Na coating on the substrate surface is likely to occur due to the pre-treatment with a NaOH solution, and thus, the Bi_2S_3 thin film has an epitaxial growth. However, studies on semiconductor thin films state that the adhesion of Na particles on the substrate produces an augmentation of the physical properties of the films [22,23].

The fact that the thickness of the films remained unchanged after the Ar plasma treatment (as shown in Fig. 2) indicates that the plasma treatment has minimal impact on the surface of the film, meaning that there is no erosion. Likewise, samples pre-treated with NaOH and subsequently treated by Ar plasma after the Bi_2S_3 deposition (sample D) have a minor roughness compared with the thermal treatment [11]. In applications such as photovoltaic device development, an absorber material with a uniform and homogeneous surface is desirable in order to ensure the creation of a continuous internal electric field. Thus, sample D displays to be the best candidate for the development of thin film solar cells based on Bi_2S_3 as absorber material.

The EDS measurements corresponding to corning glass substrate, as-prepared Bi_2S_3 thin films, and Bi_2S_3 thin films treated by Ar plasma as well as the EDS measurements of such samples pre-treated with

NaOH are displayed in Fig. 3. The atomic percentage values of elemental Na, Bi, and S, corresponding to the samples shown in Fig. 3 are given in Table 1. The results indicate that the atomic percentage of Na in the control substrate (corning glass without pre-treatment in NaOH) is 8.3 ± 0.3% whereas for the substrate pre-treated in NaOH, Na atomic percentage is 13.1 ± 0.2%. The increase in EDS peak corresponding to atomic Na in the glass substrate treated in NaOH is remarkable compared to the atomic Na present in the control substrate, as demonstrated in Fig. 3a and b. Also, in Fig. 3a, the presence of elements constituting the glass is observed, particularly Si and O; lesser extent of Ca, Mg, and Al is present. The values of Na atomic percentage for the as-prepared Bi_2S_3 thin films deposited on corning glass substrates without (Fig. 3c) and with NaOH pre-treatment (Fig. 3d) are 8.4 ± 0.3 and 9.6 ± 0.2, respectively (samples A and B). For both samples, the difference between the values of the atomic percentage of Na is only 1% as most of the Na content is removed from the substrate surface during the immersion in the reaction solution for chemical deposition of Bi_2S_3. The atomic percentage values of Na, corresponding to Bi_2S_3 thin films treated by Ar plasma, grown on corning glass substrates without (Fig. 3e) and with NaOH pre-treatment (Fig. 3f) were 8.6 ± 0.3 and 9.7 ± 0.2, respectively (samples C and D).

The atomic percentage values of Na, for samples without pre-treatment in NaOH (corning glass substrate, as-deposited Bi_2S_3 and Bi_2S_3 thin films treated by Ar-plasma) were 8.3 to 8.6 ± 0.3. This slight variation in the atomic percentage value of Na might be related to the variation in the composition of the glass substrate itself. However, for the same samples subjected to the pre-treatment in NaOH, the values of the atomic percentage of Na have presented a variation of more than 1% compared to the respective untreated samples in NaOH. Finally, it can be assumed that Na particles adhered to the surface of the glass substrate can interact with the nucleation of the film and therefore contribute in the re-crystallization of the material when Ar plasma treatment is applied.

The analysis uses the atomic percentages of Bi and S to display the stoichiometric ratios. Samples A and B have a Bi atomic percentage of 53.4% and 54.6%, respectively. Samples C and D have a Bi atomic percentage of 56.0% and 56.1%. The values in Table 1 indicate that Ar plasma treatment does not affect the thickness of ultra-thin films since they have a variation of less than 5%. The lower increment in the atomic percentage of Bi explains the increase in electrical conductivity of the films. The incident energy penetrates the Bi_2S_3 films and glass substrates, therefore the glass constituents can be seen in the measurements (Fig. 3b and f).

For the ICP-OES measurements, samples C and D were dissolved in a solution of 5% nitric acid (HNO_3). The ICP was calibrated using an aqueous analytical solution containing 5% nitric acid and 1000 μg/ml for each element (Bi, S, and Na). A solution of 5% HNO_3 was used as a blank. The presence of the elements was analyzed based on the emission peak intensity; which occurs at 588.99 nm for Na, 223 nm for Bi and 181.97 nm for S. The results are as follows: for sample (C) 5.51 μg/ml from S and 9.24 μg/ml from Bi were determined and for sample (D) 6.48 μg/ml from Na, 2.45 μg/ml from S and 9.54 μg/ml from Bi were found. These values corroborate the presence of Na in sample D, also identified by EDS measurements. However, since EDS and ICP-OES have different sensitivity values, the presence of Si, O, Al and Na was also detected by EDS, as a consequence of a greater penetration into the glass substrate. The contribution of Na, Bi and S belonging only to samples was possible by measuring ICP-OES, as demonstrated in this work.

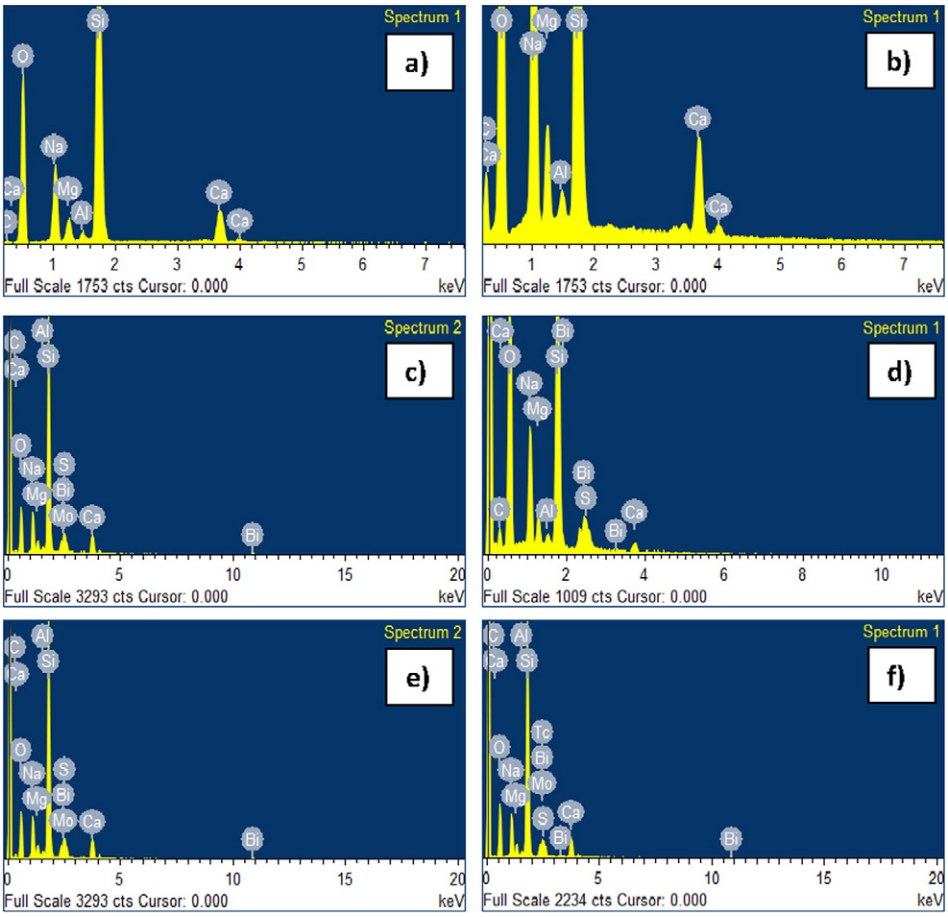

Fig. 3. EDS measurements of a) substrate corning without and b) substrate with NaOH treatment. Measuring the Bi_2S_3 as-deposited thin film c) without treatment and d) with NaOH; the Bi_2S_3 thin film d) treated by argon plasma and e) treated with NaOH and argon plasma.

4.2. Optical characterization

The optical properties of samples A, B, C, and D are shown in Fig. 4. *T*, R, and film thickness data were used to calculate the optical absorption coefficient (α). Fig. 4a shows that the samples treated with Ar plasma have a decreased transmittance of approximately 10% (at λ = 1100 nm) compared to samples without plasma treatment. Fig. 4b shows the plot of α as a function of energy (hν), which reaches values of $\alpha > 10^4\ cm^{-1}$ in the visible region, as expected for solar energy applications. Fig. 4c exhibits the plot of $(\alpha h\nu)^{2/3}$ vs. hν, which is employed to calculate E_g values by adjusting the linear part of the curve to a straight line when it approaches zero. The calculated E_g values for films in this work are: 1.68 eV and 1.67 eV for samples A and B, respectively; and 1.61 eV and 1.60 eV for samples C and D, respectively. A linear correlation (R = 0.999) was obtained for these calculations. The lower E_g value measured in sample D (1.60 eV) indicates that the Na/plasma treatments produce the most suitable E_g value for the Bi_2S_3 absorber layer. In a previous study [24], Eq. (1) was proposed for the calculation of photo-generated current density (J_L) using the spectral distribution of photon flux ($N_{p\lambda}$, $s^{-1}\ m^{-2}\ nm^{-1}$) for the values of α, as well as their wavelengths corresponding to E_g ($\lambda_g = 1240/E_g$).

$$J_L(\mathrm{mA/cm^2}) = 0.1 \times 1.602^{-19}\left[\sum_0^{\lambda_g} N_{p\lambda}(1-e^{-\alpha})\Delta\lambda\right] \quad (1)$$

We calculated the expected values of J_L and the estimated E_g values for samples A, B, C, and D by applying Eq. (1). The calculated values of J_L are as follows: 22.2 mA/cm^2, 22.3 mA/cm^2, 24.74 mA/cm^2, and 25.24 mA/cm^2, for samples A, B, C, and D, respectively. These results indicate that pre-treatment in NaOH improves the adhesion and quality of the sample, whereas the post-deposition treatment by Ar plasma results in the improvement of crystallization. Both treatments must be done in order to achieve an improved photon absorption and thus an increase in the photocurrent density generation.

4.3. Electrical characterization

The hot-point probe technique indicates that Bi_2S_3 thin films in this work are n-type. Fig. 5 shows the conductivity measurements (σ_p) of samples A, B, C, and D. Samples A and B have photoconductivity values of $6.2 \times 10^{-6}\ (\Omega\ cm)^{-1}$ and $1.2 \times 10^{-5}\ (\Omega\ cm)^{-1}$, respectively. Samples C and D have values of $5.2 \times 10^{-2}\ (\Omega\ cm)^{-1}$ and 0.277 $(\Omega\ cm)^{-1}$, respectively. The variation in the conductivity values is probably due to the change in the crystal structure from amorphous to crystalline (determined by XRD measurements), and an improvement of the surface morphology (observed by AFM). These changes in the physical properties of Bi_2S_3 thin films allowed the augmentation of charge carrier transportation through the material.

5. Conclusions

Bi_2S_3 films were obtained using the chemical bath deposition technique. XRD analysis revealed the change from the amorphous to the crystalline phases caused by the post-deposition treatment in Ar plasma. A crystalline orthorhombic structure similar to the mineral bismuthinite was observed. XRD peaks match well with the standard pattern PDF 17-0320. A crystal size of 30.5 nm for sample *D* was determined. The EDS and ICP-OES measurements proved the presence of Na in the sample *D*, which is associated to the improvement in the crystal size of the film. This study demonstrates that Bi_2S_3 films less than 100 nm in thickness, pre-treated in NaOH, and post-treated in Ar plasma exhibit improved stability and crystallinity as well as better morphological, optical, and electrical properties in comparison to non-treated films. The AFM analysis revealed films with lower roughness and less impact erosion when pre-treatment with NaOH and Ar plasma post-treatment were applied. The best E_g value is 1.60 eV for samples pre-treated in NaOH and post-treated in Ar plasma. The best photoconductivity value is 0.277 $(\Omega\ cm)^{-1}$ that corresponds to sample D (pre-treated in NaOH and post-treated in Ar-plasma). The combination of pre-treatment in NaOH and post-treatment in Ar plasma results in an increment in photoconductivity of approximately four orders of magnitude compared to the As-prepared films.

This study demonstrates that Bi_2S_3 thin films exhibit improved properties when both pre-treatment in NaOH and post-treatment in Ar

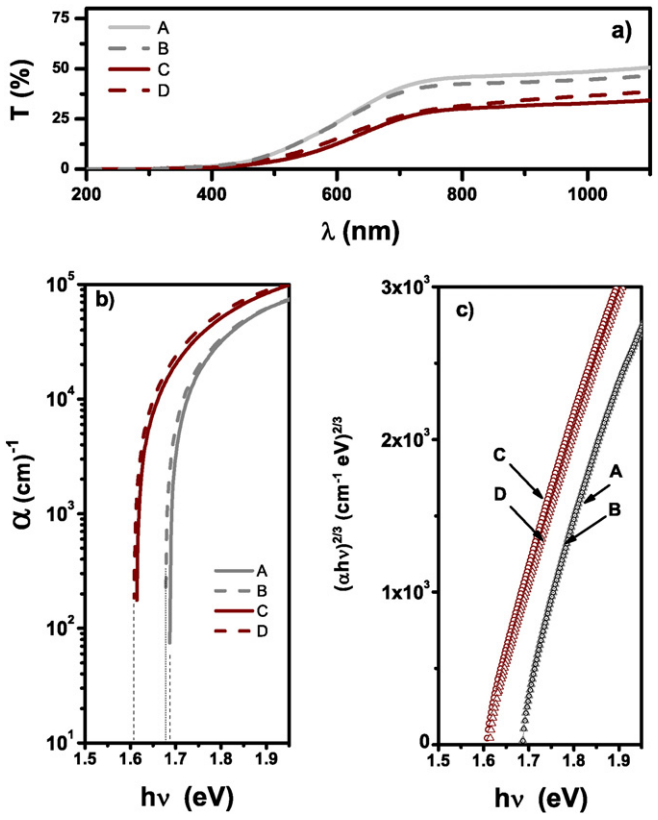

Fig. 4. a) Optical transmittance (*T*), b) optical absorption coefficient (α) and c) determination of the E_g values $(\alpha h\nu)^{2/3}$ vs. (hν) for: (A) as-prepared, (B) Na/as-prepared, (C) treated with Ar plasma, and (D) treated with Na/Ar plasma.

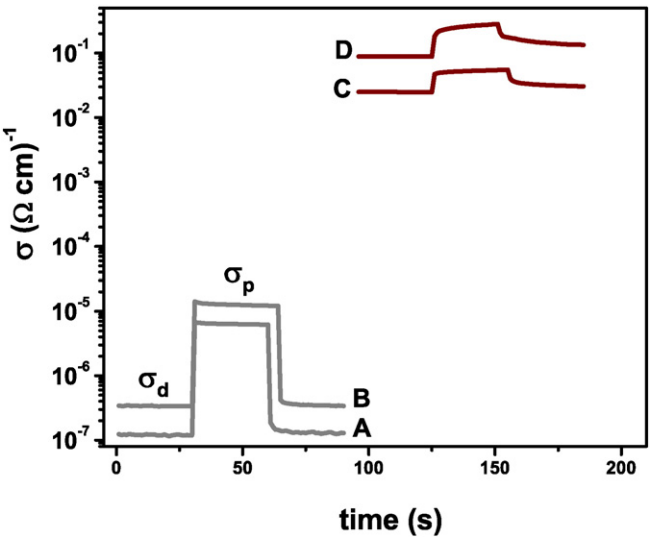

Fig. 5. Photoconductivity response plots for Bi_2S_3 thin films: (A) as-prepared, (B) Na/as-prepared, (C) treated with Ar plasma, and (D) treated with Na/Ar plasma.

plasma are applied. In consequence, we conclude that the use of plasma post-treatment as well as NaOH pre-treatment are viable methods for the enhancement of the physical properties of semiconductor ultra-thin films of Bi_2S_3 less than 100 nm in thickness.

Acknowledgments

We are grateful to Patricia E. Altuzar Coello for the GIXRD measurements, Gildardo Casarrubias for the AFM measurements, J. Campos Álvarez for electrical characterization, Oscar Gomez-Daza and Baudel García for ICP-OES measurements, and O. Flores, H. Hinojosa, and F. Castillo for technical assistance. We also want to acknowledge the support of CONACYT through the project LIFYCS-CONACYT 123122, CONACYT 225991 and CONACYT 229711. Harumi Moreno-García is grateful to DGAPA-UNAM for the postdoctoral fellowship.

References

[1] O. Madelung, Data in Science and Technology: Semiconductors Other than Group IV Elements and III–V Compounds, 50Springer–Verlag, Berlin, 1992.
[2] M. Telkes, The efficiency of thermoelectric generators I, J. Appl. Phys. 18 (1947) 1116–1127.
[3] B. Chen, C. Uher, L. Iordanidis, M.G. Kanatzidis, Transport properties of Bi_2S_3 and the ternary bismuth sulfide $KBi_{6.33}S_{10}$ and $K2Bi_8S_{13}$, Chem. Mater. 9 (1997) 1655–1658.
[4] M. Shaw, S. Holmberg, S. Kostylev, Reversible switching in thin amorphous chalcogenide films—electronic effects, Phys. Rev. Lett. 31 (1973) 542–545.
[5] R. Suarez, P.K. Nair, P.V. Kamat, Photoelectrochemical behavior of Bi_2S_3 nanoclusters and nanostructured thin films, Langmuir 14 (1998) 3236–3241.
[6] E. Pineda, M.E. Nicho, P.K. Nair, H. Hu, Optoelectronic properties of chemically deposited Bi_2S_3 thin films and the photovoltaic performance of Bi_2S_3/P3OT solar cells, Sol. Energy 86 (2012) 1017–1022.
[7] H. Yin, B. Sun, Y. Zhou, M. Wang, Z. Xu, Z. Fu, S. Ai, A new strategy for methylated DNA detection based on photoelectrochemical immunosensor using Bi_2S_3 nanorods, methyl bonding domain protein and anti-his tag antibody, Biosens. Bioelectron. 51 (2014) 103–108.
[8] L. Yongfeng, C. Hong, X. Li, Z. Gong, X. Wang, X. Peng, M. He, Z. Sheng, Wet chemical synthesis of Bi_2S_3 nanorods for efficient photocatalysis, Mater. Lett. 105 (2013) 12–15.
[9] M.E. Rincon, M. Sánchez, P.J. George, A. Sánchez, P.K. Nair, Comparison of the properties of bismuth sulfide thin films prepared by thermal evaporation and chemical bath deposition, J. Solid State Chem. 136 (1998) 167–174.
[10] R.R. Ahire, A.A. Sagade, S.D. Chavhan, V. Huse, Y.G. Gudage, F. Singh, D.K. Avasthi, D.M. Phase, R. Sharma, Modifications of structural, optical and electrical properties of nanocrystalline bismuth sulfide by using swift heavy ions, Curr. Appl. Phys. 9 (2009) 374–379.
[11] H. Moreno-García, S. Messina, M. Calixto-Rodriguez, H. Martínez, Physical properties of chemically deposited Bi_2S_3 thin films using two post-deposition treatments, Appl. Surf. Sci. 311 (2014) 729–733.
[12] A. Urbaniak, M. Igalson, F. Pianezzi, S. Bücheler, A. Chirilă, P. Reinhard, A.N. Tiwari, Effects of Na incorporation on electrical properties of Cu(In,Ga)Se_2-based photovoltaic devices on polymide substrates, Sol. Energy Mater. Sol. Cells 128 (2014) 52–56.
[13] M. Bodegård, K. Granath, A. Rockett, L. Stolt, The behavior of na implanted into Mo thin films during annealing, Sol. Energy Mater. Sol. Cells 58 (1999) 199–208.
[14] L. Stolt, J. Hedström, J. Kessler, M. Ruckh, K.O. Velthaus, H.W. Schock, ZnO/CdS/$CuInSe_2$ thin-film solar cells with improved performance, Appl. Phys. Lett. 62 (1993) 597–599.
[15] M. Ruckh, D. Schmid, M. Kaiser, R. Schäffler, T. Walter, H.W. Schock, Influence of substrates on the electrical properties of Cu(In, Ga)Se_2 thin films, Proceedings of the 1994 IEEE First World Conference on Photovoltaic Energy Conversion 1994, pp. 156–159.
[16] M. Bodegård, L. Stolt, J. Hedström, The influence of sodium on the grain structure of $CuInSe_2$ films for photovoltaic applications, Proceedings of the 12th European Photovoltaic Solar Energy Conference 1994, pp. 1743–1746.
[17] M. Lammer, U. Klemm, M. Powalla, Sodium co-evaporation for low temperature Cu(In, Ga)Se_2 deposition, Thin Solid Films 387 (2001) 33–36.
[18] A. Rockett, J.S. Britt, T. Gillespie, C. Marshall, M.M. Al-Jassim, F. Hasoon, R. Matson, B. Basol, Na in selenized Cu(In, Ga)Se_2 on Na containing and Na-free glasses distribution, grain structure and device performances, Thin Solid Films 372 (2000) 212–217.
[19] M.T.S. Nair, P.K. Nair, Photoconductive bismuth sulfide thin films by chemical deposition, Semicond. Sci. Technol. 5 (1990) 1225–1230.
[20] M.E. Rincón, M. Sánchez, P.J. George, A. Sánchez, P.K. Nair, Comparison of the properties of bismuth sulfide thin films prepared by thermal evaporation and chemical bath deposition, J. Solid State Chem. 136 (1998) 167–174.
[21] D.K. Schroder, Semiconductor Material and Device Characterization, 3r ed. John Wiley & Sons, Hoboken, 2006.
[22] M. Zribi, M. Kanzari, B. Rezig, Post-growth annealing treatment effects on properties of Na doped $CuInS_2$ thin films, Mater. Sci. Eng. B 149 (2008) 1–6.
[23] A. Urbaniak, M. Igalson, F. Pianezzi, S. Bücjeler, A. Chirila, P. Reinhard, A.N. Tiwari, Effects of Na incorporation on electrical properties of Cu(In, Ga)Se_2-based photovoltaic devices on polymide substrates, Sol. Energy Mater. Sol. Cells 128 (2014) 52–56.
[24] H. Moreno-García, M.T.S. Nair, P.K. Nair, Chemically deposited lead sulfide and bismuth sulfide thin films and Bi_2S_3/PbS solar cells, Thin Solid Films 519 (2011) 2287–2295.